Effects of acetylation on the thermal decomposition kinetics of makino bamboo fibers

Yu-Shan Jhu, Ke-Chang Hung, Jin-Wei Xu & Jyh-Horng Wu

Wood Science and Technology
Journal of the International Academy of Wood Science

ISSN 0043-7719
Volume 53
Number 4

Wood Sci Technol (2019) 53:873-887
DOI 10.1007/s00226-019-01105-z

Springer

Wood Science and Technology (2019) 53:873–887
https://doi.org/10.1007/s00226-019-01105-z

ORIGINAL

Effects of acetylation on the thermal decomposition kinetics of makino bamboo fibers

Yu-Shan Jhu[1] · Ke-Chang Hung[1] · Jin-Wei Xu[1] · Jyh-Horng Wu[1]

Received: 4 December 2018 / Published online: 6 June 2019

Abstract

In this study, makino bamboo (*Phyllostachys makinoi*) fibers were acetylated with different solution ratios of acetic anhydride/dimethylformamide using a liquid phase reaction. This reaction resulted in the production of acetylated bamboo fibers (BFs) with the following weight percent gains (WPGs): 2, 6, 9, 13, and 19%. The effects of the acetylation level on the thermal decomposition kinetics of bamboo fibers were evaluated by thermogravimetric analysis. The results revealed that as the acetylation level increased, both the onset and maximum decomposition temperatures increased. In addition, four model-free iso-conversional methods, the Friedman method, Flynn–Wall–Ozawa method, the Starink method, and the modified Coats–Redfern method, were used to determine the thermal decomposition kinetics. Accordingly, the activation energies of thermal decomposition with conversion rates ranging between 10% and 70% were 191–196, 190–191, 192–194, 182–186, 186–191, and 189–201 kJ/mol for unmodified BFs and acetylated BFs with WPGs of 2, 6, 9, 13, and 19%, respectively. There were no significant dependencies among them. Furthermore, the Avrami method was used to determine the reaction order of unmodified BFs (0.47), which was lower than those of acetylated BFs (0.55–0.74).

Introduction

In recent years, thermoplastics reinforced with natural fibers (NFs) have been of significant interest and have attracted significant attention for the use as alternative materials to solid wood and some plastic products. These NF characteristics can mitigate the disadvantages of polymer matrices, as their incorporation has produced polymer composites with several advantages, including low density, low equipment abrasiveness, high stiffness, high specific strength, renewability, biodegradability,

Yu-Shan Jhu and Ke-Chang Hung contributed equally to this work.

✉ Jyh-Horng Wu
eric@nchu.edu.tw

[1] Department of Forestry, National Chung Hsing University, Taichung 402, Taiwan

and relatively low cost (Zhang et al. 2002; Lee et al. 2010; Kumar et al. 2011; Migneault et al. 2011; Dittenber and Ganga Rao 2012; Liu et al. 2014, 2015; Saba et al. 2015). However, despite these advantages, the applicability of wood–plastic composites (WPCs) remains limited by the hygroscopicity and incompatibility between hydrophilic lignocellulosics and hydrophobic thermoplastics. Therefore, over the past few decades, several physical and chemical approaches, including esterification, thermal treatment, and the addition of coupling agents, have been used to increase the hydrophobicity of lignocellulosic materials and improve their dimensional and thermal stabilities (Rowell 1983; Li et al. 2007; Hung and Wu 2010; Hung et al. 2015; Pelaez-Samaniego et al. 2013). Among these approaches, NF esterification has received the most attention, and acetylation with acetic anhydride (AA) has been the most commonly and widely used method. The surface energy of acetylated NFs is much closer to that of a polymer matrix and produces better wettability and interfacial interactions with the matrix (Li et al. 2007; Ou et al. 2010), which are properties that improve the dimensional stability and mechanical properties of the resulting composites (Rowell 1983; Tronc et al. 2007; Gardea-Hernández et al. 2008).

Furthermore, NFs are susceptible to thermal degradation during the composite fabrication process (Saheb and Jog 1999). As a result, the thermal degradation of NF is one of the most influential factors concerning the properties of composites. Thus, a thorough understanding of the thermal decomposition process of NFs could aid in the development of composites (Yao et al. 2008; Li et al. 2013). In addition, acetylation is an effective method used to improve the thermal stability of NFs (Wu et al. 2004). Usually, the thermal stability of acetylated NFs is estimated by thermogravimetric analysis (TGA). Meanwhile, activation energy is one of the key parameters used to describe the thermal decomposition behavior of the polymer and NFs. However, the effects of the acetylation level on the activation energy of thermal decomposition of NFs have not yet been assessed. Therefore, in order to fill this gap, this study used dynamic TGA to analyze the thermal decomposition kinetics of acetylated bamboo fibers (BFs), and the activation energy of the thermal decomposition of the acetylated BFs was determined by various model-free iso-conversional methods, including the Friedman, Flynn–Wall–Ozawa (F–W–O), Starink, and modified Coats–Redfern (modified C–R) methods (Yao et al. 2008; Gai et al. 2013).

Materials and methods

Materials

BFs were prepared from a 3-year-old makino bamboo (*Phyllostachys makinoi* Hayata), which was provided by a local bamboo-processing factory and hammer-milled and sieved to obtain particles with a size range of 24 to 30 mesh (φ 550–700 μm). All samples were extracted with acetone using a Soxhlet apparatus for 24 h and then washed with distilled water and dried at 105 °C for 12 h. The chemicals and solvents used in this experiment were purchased from Sigma-Aldrich Chemical Co. (St. Louis, MO, USA).

Acetylation

BFs were acetylated with AA/dimethylformamide (DMF) using a conventional liquid phase reaction (Yang et al. 2014). Oven-dried BFs were immersed in different AA/DMF solutions (1/99, 1.5/98.5, 5/95, 10/90, and 20/80 AA/DMF (v/v)) at a solid/liquid ratio of 0.05 g/ml to obtain acetylated BFs with different degrees of modification. The reaction was stirred at 140 °C for 2 h, and all reaction conditions are presented in Table 1. At the end of the reactions, the acetylated BFs were washed with distilled water and Soxhlet-extracted with acetone for 4 h. Finally, the acetylated BFs were dried at 105 °C for 12 h. The weight percent gain (WPG) of the BFs was calculated based on the oven-dried method.

Thermogravimetric analysis

A PerkinElmer Pyris 1 thermogravimetric analyzer (Buckinghamshire, UK) was used to study the thermal properties of unmodified and acetylated BFs. Measurements on 3 mg samples were performed in a nitrogen atmosphere (20 ml/min) at temperatures ranging from 50 to 600 °C. The heating rate was set at 2.5, 5, 10, 20, or 30 °C/min. The data obtained were used to calculate the kinetic parameters by model-free iso-conversional methods. The conversion rate α is defined as:

$$\alpha = (W_0 - W_t)/(W_0 - W_f) \tag{1}$$

where W_0 is the initial weight of the sample, W_f is the final residual weight, and W_t is the weight of the oxidized or pyrolyzed sample at time t. The common iso-conversional methods used in this study included the following methods: the Friedman (Eq. 2), F–W–O (Eq. 3), modified C–R (Eq. 4), and Starink (Eq. 5) method. The equations used for these methods are as follows:

$$\ln(\mathrm{d}\alpha/\mathrm{d}t) = \ln\left[Af(\alpha)\right] - E_a/(RT) \tag{2}$$

$$\log\beta = \log\left[AE_a/(Rg(\alpha))\right] - 2.315 - 0.4567E_a/(RT) \tag{3}$$

$$\ln\left\{\beta/\left[T^2\left(1 - 2RT/E_a\right)\right]\right\} = \ln\left\{-AR/\left[E_a \ln(1-\alpha)\right]\right\} - E_a/(RT) \tag{4}$$

$$\ln(\beta/T^{1.8}) = C_s - 1.0037\left(E_a/RT\right) \tag{5}$$

Table 1 Reaction conditions for different acetylated BFs

Acetylated BFs	BFs/AA (g/ml)	Reaction temperature (°C)	Reaction time (h)	WPG (%)
WPG 2	1/0.2	140	2	2.3 ± 0.9
WPG 6	1/0.3	140	2	5.9 ± 1.1
WPG 9	1/1	140	2	8.7 ± 1.6
WPG 13	1/2	140	2	12.7 ± 0.8
WPG 19	1/4	140	2	19.0 ± 1.5

Values are the mean ± SD ($n = 5$)

where α is the conversion rate, A is the pre-exponential factor (min^{-1}), $f(\alpha)$ is the reaction model, E_a is the apparent activation energy (kJ/mol), R is the gas constant (8.314 J/K/mol), T is the absolute temperature (K), β is the heating rate, $g(\alpha)$ is a function of the conversion and C_s is a constant (Yao et al. 2008; Gai et al. 2013; Li et al. 2013). Therefore, for a given conversion fraction, a linear relationship was produced by plotting $\ln(d\alpha/dt)$, $\log\beta$, $\ln(\beta/T^2)$ and $\ln(\beta/T^{1.8})$ versus $1/T$ at different heating rates. E_a was then calculated from the slope of the resulting straight line (Yao et al. 2008; Gai et al. 2013; Li et al. 2013).

In addition to the apparent activation energy, reaction order is an important parameter used to investigate thermal decomposition kinetics (Gai et al. 2013). The Avrami theory was used to determine the reaction order in this study using the following equation (Eq. 6):

$$\ln\left[-\ln\left(1-\alpha\right)\right] = \ln A - E_a/RT - n\ln\beta \tag{6}$$

where n represents reaction order. For a given temperature, a linear relationship was produced by plotting $\ln[-\ln(1-\alpha)]$ versus $\ln\beta$ at different temperature heating rates, and the reaction order was deduced from the slope of the resulting line (Gai et al. 2013).

Analysis of variance

All the results were expressed as the mean ± SD. The significance of the differences was calculated using Scheffe's test, and $p < 0.05$ was considered to be significant.

Results and discussion

Thermal stability properties

Figure 1 shows the TGA and DTG curves of unmodified BFs and acetylated BFs produced with different WPGs at a heating rate of 10 °C/min. The TGA curve of unmodified BFs exhibited a gradual increase in weight loss (WL) above 250 °C (Fig. 1a), and the DTG curve (Fig. 1b) of unmodified BFs illustrated a maximum WL rate at 348 °C. In contrast, all acetylated BFs showed significant WL at temperatures above 300 °C, and all maximum WL rates occurred at a higher temperature range, 366–371 °C. It is well known that thermally instable hemicelluloses are primarily responsible for the initial phase of wood thermal degradation (Boonstra and Tjeerdsma 2006; Chaouch et al. 2010; Wang et al. 2012). This result indicated that the thermal stability of BFs could be effectively enhanced with acetylation. Similar results were obtained by Xu et al. (2010) and Wei et al. (2013). Furthermore, Bledzki et al. (2008) reported that the increase in the thermal stability of acetylated NFs could be due to the removal of wax, pectin, and extractive components from the fiber surface during acetylation. Additionally, the solid residue of all acetylated BFs (13.0–15.3%) was lower than that of the unmodified BFs (21.0%) at 600 °C. The acyl groups in the acetylated BF could have been eliminated with the volatile products and, thus, were not converted to char (Wu et al. 2004; Hung et al. 2017).

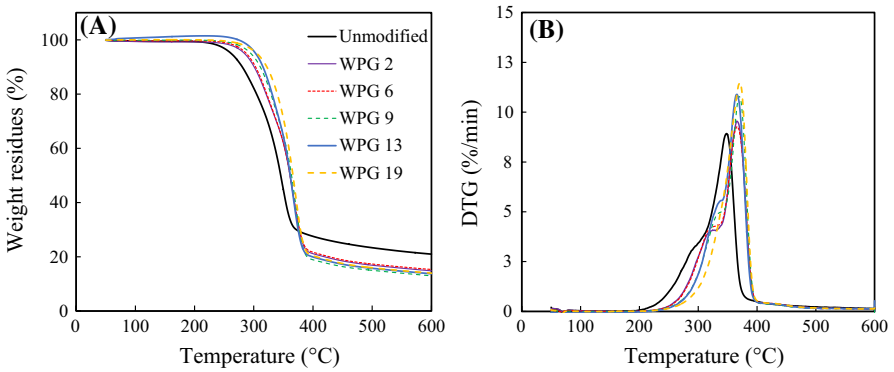

Fig. 1 TGA (**a**) and DTG (**b**) curves of unmodified and acetylated bamboo fibers with various WPGs (heating rate: 10 °C/min)

Thermal decomposition kinetics analysis

To understand the thermal decomposition kinetics of unmodified and acetylated BFs in depth, model-free iso-conversional methods were applied for TG data evaluation. The plots of iso-conversional Friedman, F–W–O, Starink, and modified C–R methods showed a general trend upon determining the E_a. Examples of typical plots based on the Friedman model and regression lines for unmodified and acetylated BFs are presented in Fig. 2. The calculated E_a and corresponding R^2 values are also presented in Table 2. It is remarkable that most R^2 values were higher than 0.99. Thus, the Friedman method was suitable for determining the E_a of unmodified and acetylated BFs. As shown in Table 2, the E_a values of unmodified BFs were between 167 and 212 kJ/mol for conversion rates of 10–70%. Furthermore, E_a values increased markedly as conversion rates increased to 40%. Accordingly, these results indicated that the thermal decomposition of BFs at different conversion rates proceeded with varied reaction mechanisms. A similar trend was reported by Oza et al. (2014). This phenomenon could also be explained by the thermogravimetric analysis of DTG curves. The thermal decomposition temperatures for conversions with conversion rates of 10–30% ranged from 274 to 312 °C for unmodified BFs when a heating rate of 10 °C/min was used, while the highest thermal decomposition rate (DTG peak temperature) occurred at 348 °C, as shown in Fig. 1b. In this temperature range, the hemicellulose should have been decomposed almost completely; lignin should have continued to decompose slowly because the pyrolysis of hemicellulose, cellulose, and lignin occurred primarily at 220–315 °C, 315–400 °C, and 160–900 °C, respectively (Yang et al. 2007). In other words, the hemicellulose and lignin were primarily responsible for conversions below 40%, and the contents of both components decreased as conversion rates increased. In addition, Gronli et al. (2002) and Yao et al. (2008) reported that the activation energies of hemicellulose, cellulose, and lignin were 105–111, 195–213, and 35–65 kJ/mol, respectively. Therefore, the thermal decomposition behaviors of BFs were significantly different

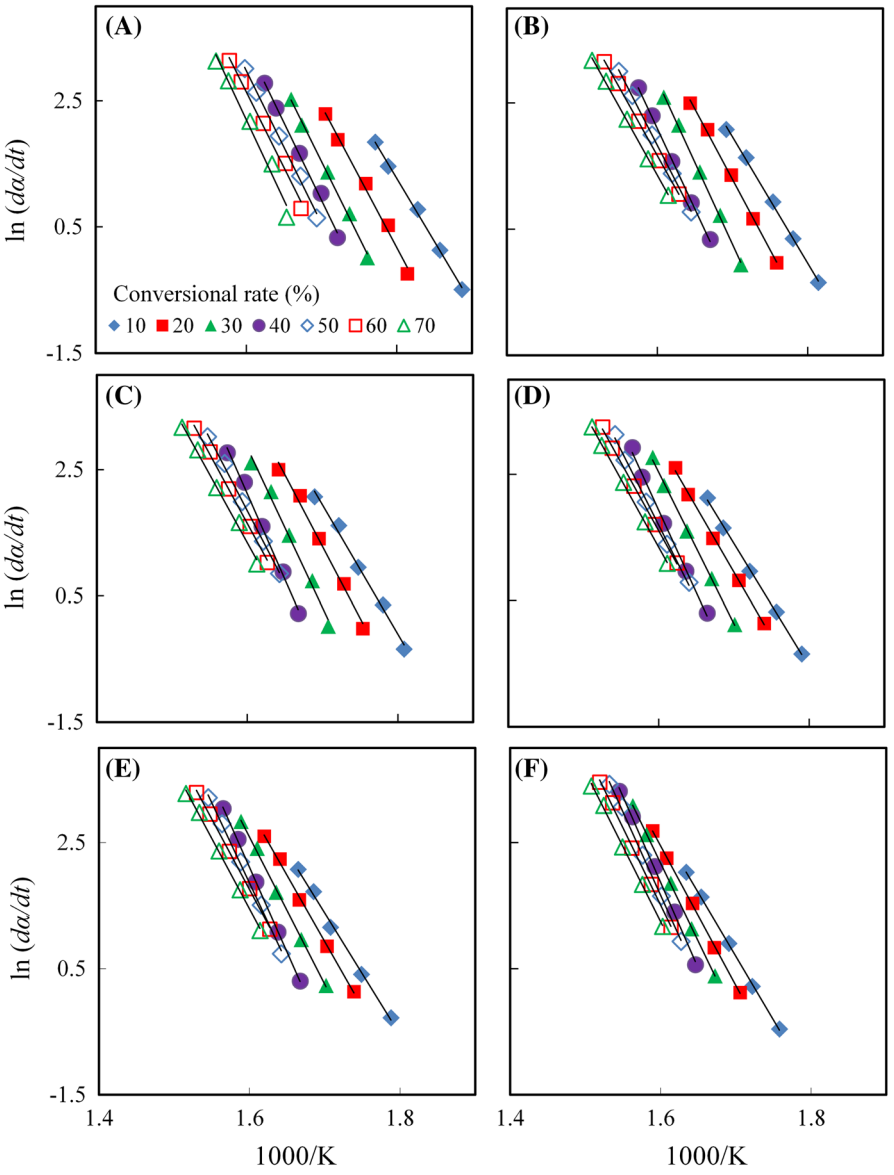

Fig. 2 Typical iso-conversional Friedman method plots for unmodified bamboo fibers (**a**) and WPG 2 (**b**), WPG 6 (**c**), WPG 9 (**d**), WPG 13 (**e**), and WPG 19 (**f**) acetylated bamboo fibers

when conversions were below 40%. Furthermore, the results of all acetylated BFs presented similar trends to those of unmodified BFs. The E_a values of acetylated BFs calculated by the Friedman method with conversion rates of 10–70% were 166–216, 167–226, 162–217, 160–224, and 168–226 kJ/mol for WPGs of 2, 6, 9, 13, and 19%, respectively.

Table 2 Apparent activation energies of unmodified and various acetylated bamboo fibers calculated by the Friedman method

Samples	Items	Conversion rates							
		10%	20%	30%	40%	50%	60%	70%	Mean
Unmodified	E_a (kJ/mol)	167	187	200	205	201	199	212	196
	R^2	0.998	0.993	0.997	0.996	0.998	0.993	0.980	–
WPG 2	E_a (kJ/mol)	166	186	216	213	193	178	178	190
	R^2	0.998	0.999	0.999	0.999	~1	0.999	0.999	–
WPG 6	E_a (kJ/mol)	167	189	211	226	191	183	180	192
	R^2	0.992	0.991	0.991	0.996	0.998	0.998	0.995	–
WPG 9	E_a (kJ/mol)	162	172	199	217	197	179	178	186
	R^2	0.999	0.999	0.999	0.997	0.998	0.999	~1	–
WPG 13	E_a (kJ/mol)	160	174	195	224	211	186	185	191
	R^2	0.997	0.998	0.999	~1	0.998	0.999	0.998	–
WPG 19	E_a (kJ/mol)	168	184	206	226	219	204	198	201
	R^2	~1	~1	~1	0.998	0.999	0.998	0.999	–

On the other hand, the typical plots based on the F–W–O, Starink, and modified C–R models for unmodified BFs are presented in Fig. 3. The plots were similar to those produced by the Friedman model, and the results indicated those methods were also suitable for determining the E_a of unmodified BFs. Furthermore, the acetylated BF plots (not shown) were similar to those presented in Fig. 3, and the E_a and corresponding R^2 values are listed in Table 3. The E_a change trends of the F–W–O, Starink, and modified C–R methods were similar to the results from the Friedman approach for unmodified and acetylated BFs. In addition, the average E_a values calculated using conversion rates of 10–70% were 191, 191, 194, 182–183, 186, and 189–190 kJ/mol for unmodified BFs and acetylated BFs with WPGs of 2, 6, 9, 13, and 19%, respectively. Notably, the values calculated by the F–W–O, Starink, and modified C–R methods were different from those calculated by the Friedman method. However, the activation energies only provided information regarding the minimum energy required to break the chemical bonds between atoms. Therefore, the different kinetic analysis methods used in this study were complementary rather than competitive (Brown et al. 2000; Yao et al. 2008) and aided in understanding the effects of acetylation on the thermal decomposition behavior of BFs. Accordingly, acetylation was demonstrated to effectively improve the thermal stability of BFs, but it did not affect the E_a value of the thermal decomposition, which was calculated by model-free iso-conversional methods.

To further understand the dependence of reaction order on the decomposition temperature during the primary thermal decomposition process, seven decomposition temperatures (with conversion rates between 10% and 70%) were employed using five heating rates (2.5, 5, 10, 20, and 30 K/min). The regression lines of unmodified and acetylated BFs were determined using the Avrami theory and are illustrated in Fig. 4. The calculated reaction orders and corresponding R^2 values (most values were higher than 0.99) are also listed in Table 3. The results

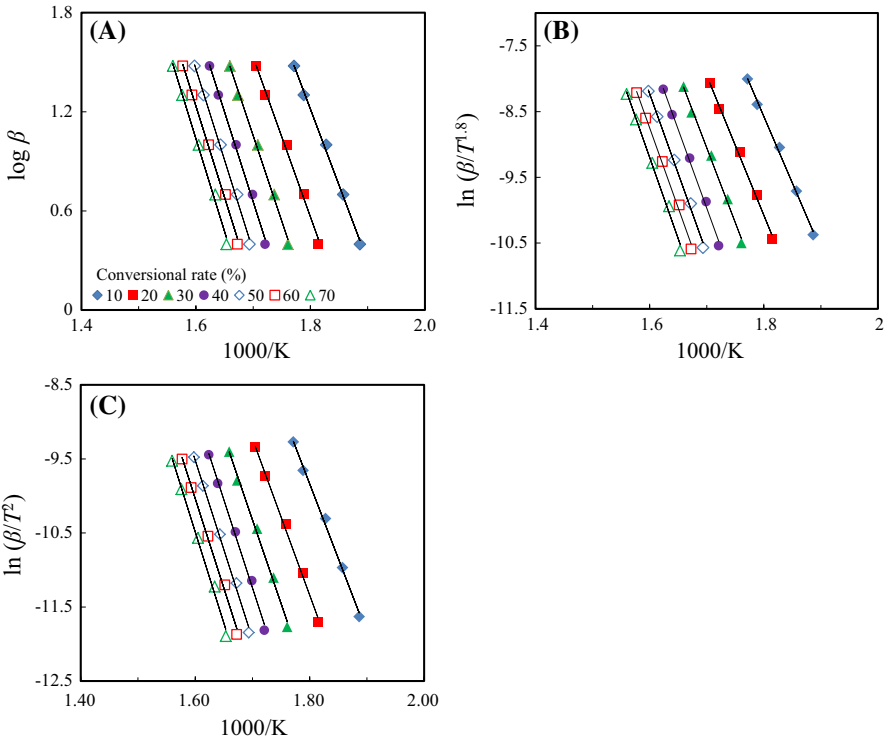

Fig. 3 Typical iso-conversional F–W–O (**a**), Starink (**b**), and modified C–R (**c**) method plots of unmodified bamboo fibers

revealed a higher reaction order occurred during the initial stage (conversion rate < 30%) of thermal decomposition for unmodified and acetylated BFs, with the exception of acetylated BFs with a WPG of 19%, which showed a more consistent reaction order during the thermal decomposition process. Several studies have investigated the reaction order of the thermal decomposition of three main components of biomass (Antal et al. 1998; Manyà et al. 2003; Mészáros et al. 2004; Huang et al. 2011). According to these previous studies, the thermal decomposition of cellulose, hemicellulose, and lignin can be described by first-, second-, and third-order reactions, respectively. The thermal decomposition temperatures of hemicellulose and lignin were lower than that of cellulose, resulting in a higher reaction order during the initial stage of BF thermal decomposition. The reaction orders for conversion rates of 10–70% were 0.41–0.58, 0.44–0.74, 0.44–0.70, 0.58–0.82, 0.60–0.78, and 0.71–0.78 for unmodified BFs and acetylated BFs with WPGs of 2, 6, 9, 13, and 19%, respectively (Table 3). The reaction order of unmodified BFs was similar to the reaction order of wood waste reported by Vuthaluru (2004), which was 0.42.

Table 3 Apparent activation energy and reaction order of unmodified and various acetylated bamboo fibers calculated by the F–W–O, modified C–R, and Starink methods and Avrami theory

Specimen	Methods	Items	Conversion rates							
			10%	20%	30%	40%	50%	60%	70%	Mean
Unmodified	F–W–O	E_a (kJ/mol)	168	176	188	198	201	201	204	191
		R^2	0.997	0.996	0.996	0.997	0.997	0.996	0.995	–
	Modified C–R	E_a (kJ/mol)	167	175	188	198	201	201	205	191
		R^2	0.996	0.995	0.995	0.996	0.996	0.996	0.994	–
	Starink	E_a (kJ/mol)	168	176	188	198	201	201	205	191
		R^2	0.996	0.995	0.995	0.996	0.996	0.996	0.994	–
	Avrami theory	Reaction order	0.58	0.52	0.45	0.41	0.42	0.44	0.48	0.47
		R^2	0.994	0.990	0.985	0.991	0.998	0.999	0.998	–
WPG 2	F–W–O	E_a (kJ/mol)	164	174	194	208	205	199	195	191
		R^2	0.994	0.998	0.999	0.999	0.999	0.999	0.999	–
	Modified C–R	E_a (kJ/mol)	163	173	194	208	205	199	194	191
		R^2	0.994	0.998	0.999	0.999	0.999	0.999	0.999	–
	Starink	E_a (kJ/mol)	163	173	194	208	205	199	195	191
		R^2	0.994	0.998	0.999	0.999	0.999	0.999	0.999	–
	Avrami theory	Reaction order	0.74	0.71	0.60	0.48	0.44	0.46	0.50	0.56
		R^2	0.983	0.989	0.981	0.970	0.988	0.993	0.988	–

Table 3 (continued)

Specimen	Methods	Items	Conversion rates							
			10%	20%	30%	40%	50%	60%	70%	Mean
WPG 6	F–W–O	E_a (kJ/mol)	169	178	194	209	207	203	198	194
		R^2	0.989	0.991	0.990	0.992	0.994	0.996	0.997	–
	Modified C–R	E_a (kJ/mol)	168	177	194	210	208	203	198	194
		R^2	0.988	0.990	0.989	0.991	0.993	0.996	0.997	–
	Starink	E_a (kJ/mol)	168	178	194	210	208	203	198	194
		R^2	0.988	0.990	0.989	0.991	0.993	0.996	0.997	–
	Avrami theory	Reaction order	0.70	0.68	0.58	0.47	0.44	0.46	0.50	0.55
		R^2	0.968	0.974	0.965	0.950	0.973	0.990	0.991	–
WPG 9	F–W–O	E_a (kJ/mol)	156	165	178	195	198	196	194	183
		R^2	~1	0.999	0.999	0.999	0.999	0.999	0.999	–
	Modified C–R	E_a (kJ/mol)	155	164	177	195	198	195	193	182
		R^2	~1	0.999	0.999	0.999	0.999	0.999	0.999	–
	Starink	E_a (kJ/mol)	155	164	177	195	198	196	194	183
		R^2	~1	0.999	0.999	0.999	0.999	0.999	0.999	–
	Avrami theory	Reaction order	0.82	0.79	0.73	0.64	0.58	0.58	0.59	0.68
		R^2	0.993	0.998	0.995	0.987	0.994	0.998	0.992	–

Table 3 (continued)

Specimen	Methods	Items	Conversion rates							
			10%	20%	30%	40%	50%	60%	70%	Mean
WPG 13	F–W–O	E_a (kJ/mol)	160	166	177	195	204	203	200	186
		R^2	0.990	0.996	0.998	0.998	0.999	~1	~1	–
	Modified C–R	E_a (kJ/mol)	158	165	176	195	204	203	200	186
		R^2	0.988	0.996	0.997	0.998	0.999	~1	~1	–
	Starink	E_a (kJ/mol)	159	165	176	195	205	204	200	186
		R^2	0.989	0.996	0.997	0.998	0.999	~1	~1	–
	Avrami theory	Reaction order	0.78	0.77	0.74	0.66	0.60	0.60	0.62	0.68
		R^2	0.872	0.975	0.996	0.993	0.993	0.996	0.993	–
WPG 19	F–W–O	E_a (kJ/mol)	159	170	181	194	207	209	209	190
		R^2	~1	0.999	0.999	0.999	~1	~1	~1	–
	Modified C–R	E_a (kJ/mol)	158	169	180	194	207	209	209	189
		R^2	0.999	0.999	0.999	0.999	~1	~1	~1	–
	Starink	E_a (kJ/mol)	158	169	180	194	207	209	209	190
		R^2	0.999	0.999	0.999	0.999	~1	~1	~1	–
	Avrami theory	Reaction order	0.78	0.75	0.74	0.71	0.71	0.73	0.76	0.74
		R^2	0.992	0.998	0.998	0.996	0.997	0.998	0.999	–

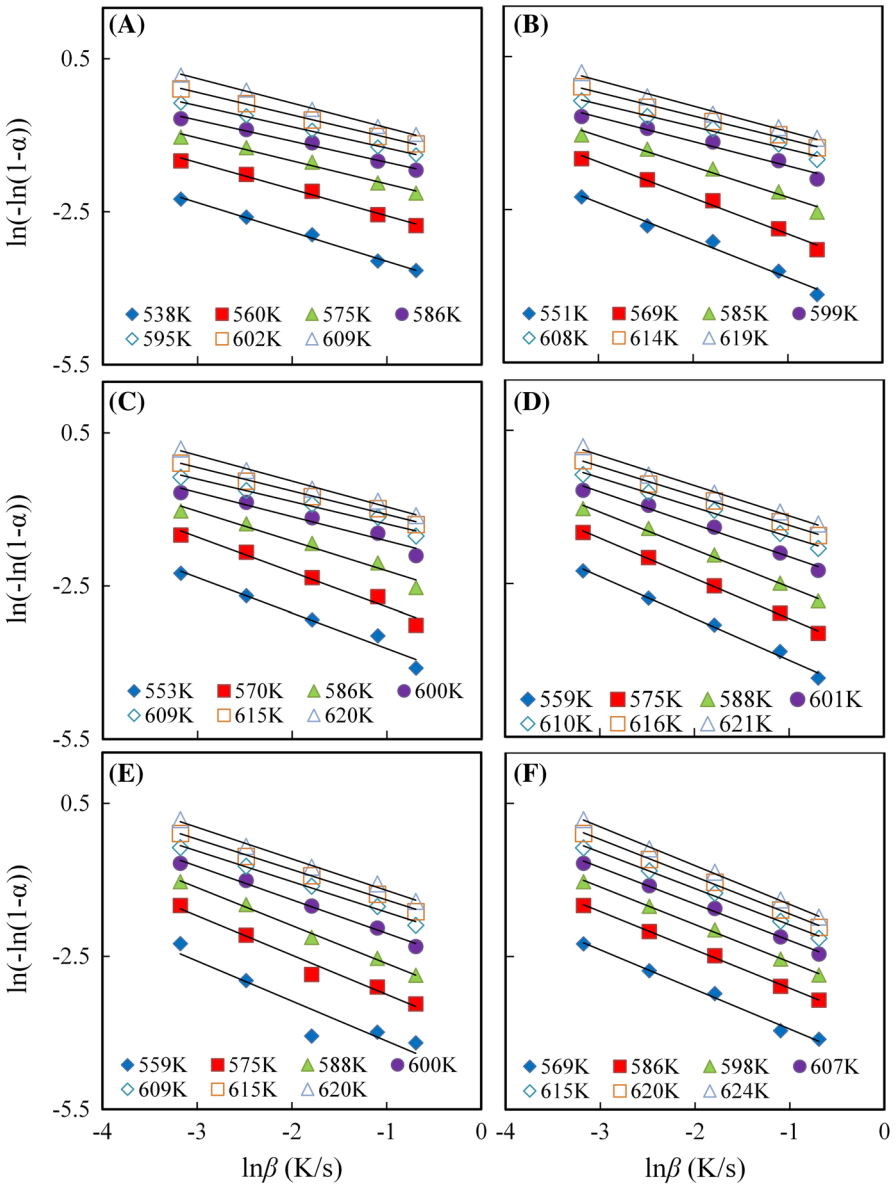

Fig. 4 Regression lines/reaction orders determined by the Avrami theory for unmodified bamboo fibers (**a**) and WPG 2 (**b**), WPG 6 (**c**), WPG 9 (**d**), WPG 13 (**e**), and WPG 19 (**f**) acetylated bamboo fibers

Conclusion

This study presented the thermal decomposition kinetics of unmodified and acetylated bamboo fibers (BFs) with various weight percent gains (WPGs) of 2, 6, 9, 13, and 19% by dynamic TG analysis. The results showed that the thermal

decomposition temperature of BFs could effectively be enhanced through acetylation. In addition, the apparent activation energy (E_a) value of all BFs increased markedly with increasing conversion rates up to 40%, indicating the thermal decomposition of BFs at different conversion rates should proceed with varied reaction mechanisms. However, the average E_a of unmodified BFs (191–196 kJ/mol) was not significantly different from the acetylated BFs (182–201 kJ/mol) at conversion rates of 10–70% when determined by the following four model-free iso-conversional methods: the Friedman method, the Flynn–Wall–Ozawa (F–W–O) method, the Starink method, and the modified Coats–Redfern (modified C–R) method. The reaction orders of unmodified BFs and acetylated BFs with WPGs of 2, 6, 9, 13, and 19% were 0.41–0.58, 0.44–0.74, 0.44–0.70, 0.58–0.82, 0.60–0.78, and 0.71–0.78, respectively.

Acknowledgements This work was financially supported by a research grant from the Ministry of Science and Technology, Taiwan (MOST 106-2628-B-005-008-CC3).

References

Antal MJ, Varhegyi G, Jakab E (1998) Cellulose pyrolysis kinetics: revisited. Ind Eng Chem Res 37(4):1267–1275. https://doi.org/10.1021/ie970144v

Bledzki A, Wu K, Mamum AA, Lucka-Gabor M, Gutowski VS (2008) The effects of acetylated on properties of flex fiber and its polypropylene composites. Express Polym Lett 2(6):413–422. https://doi.org/10.3144/expresspolymlett.2008.50

Boonstra MJ, Tjeerdsma B (2006) Chemical analysis of heat treated softwoods. Eur J Wood Prod 64:204–211. https://doi.org/10.1007/s00107-005-0078-4

Brown ME, Maciejewski M, Vyazovkin S, Nomen R, Sempere J, Burnham A (2000) Computational aspects of kinetic analysis. Part A: the ICTAC kinetics project-data, methods and results. Thermochim Acta 355:125–143. https://doi.org/10.1016/S0040-6031(00)00443-3

Chaouch M, Pétrissans M, Pétrissans A, Gérardin P (2010) Use of wood elemental composition to predict heat treatment intensity and decay resistance of different softwood and hardwood species. Polym Degrad Stab 95:2255–2259. https://doi.org/10.1016/j.polymdegradstab.2010.09.010

Dittenber DB, Ganga Rao HVS (2012) Critical review of recent publications on use of natural composites in infrastructure. Compos Part A-Appl S 43:1419–1429. https://doi.org/10.1016/j.compositesa.2011.11.019

Gai C, Dong Y, Zhang T (2013) The kinetic analysis of the pyrolysis of agricultural residue under non-isothermal conditions. Bioresour Technol 127:298–305. https://doi.org/10.1016/j.biortech.2012.09.089

Gardea-Hernández G, Ibarra-Gómez R, Flores-Gallardo SG, Hernández-Escobar CA, Pérez-Romo P, Zaragoza-Contreras EA (2008) Fast wood fiber esterification. I. Reaction with oxalic acid and cetyl alcohol. Carbohydr Polym 71:1–8. https://doi.org/10.1016/j.carbpol.2007.05.014

Gronli MG, Verhegyi G, Di Blasi C (2002) Thermogravimetric analysis and devolatilization kinetics of wood. Ind Eng Chem Res 41:4201–4208. https://doi.org/10.1021/ie0201157

Huang YF, Kuan WH, Chiueh PT, Lo SL (2011) A sequential method to analyze the kinetics of biomass pyrolysis. Bioresour Technol 102:9241–9246. https://doi.org/10.1016/j.biortech.2011.07.015

Hung KC, Wu JH (2010) Mechanical and interfacial properties of plastic composite panels made from esterified bamboo particles. J Wood Sci 56:216–221. https://doi.org/10.1007/s10086-009-1090-9

Hung KC, Wu TL, Chen YL, Wu JH (2015) Assessing the effect of wood acetylation on mechanical properties and extended creep behavior of wood/recycled-polypropylene composites. Constr Build Master 108:139–145. https://doi.org/10.1016/j.conbuildmat.2016.01.039

Hung KC, Yang CN, Yang TC, Wu TL, Chen YL, Wu JH (2017) Characterization and thermal stability of acetylated slicewood production by alkali-catalyzed esterification. Materials 10:393–406. https://doi.org/10.3390/ma10040393

Kumar V, Tyagi L, Sinha S (2011) Wood flour—reinforced plastic composites: a review. Rev Chem Eng 27:253–264. https://doi.org/10.1515/REVCE.2011.006

Lee CH, Wu TL, Chen YL, Wu JH (2010) Characteristics and discrimination of five types of wood–plastic composites by Fourier transform infrared spectroscopy combined with principal component analysis. Holzforschung 64:699–704. https://doi.org/10.1515/HF.2010.104

Li X, Tabil LG, Panigrahi S (2007) Chemical treatments of natural fiber for use in natural fiber-reinforced composite: a review. J Polym Environ 15:25–33. https://doi.org/10.1007/s10924-006-0042-3

Li Y, Du L, Kai C, Huang R, Wu Q (2013) Bamboo and high density polyethylene composite with heat-treated bamboo fiber: thermal decomposition properties. BioResources 8(1):900–912. https://doi.org/10.15376/biores.8.1.900-912

Liu W, Chen T, Wen X, Qiu R, Zhang X (2014) Enhanced mechanical properties and water resistance of bamboo fiber—unsaturated polyester composites coupled by isocyanatoethyl methacrylate. Wood Sci Technol 48:1241–1255. https://doi.org/10.1007/s00226-014-0668-6

Liu W, Huang J, Wang N, Lei S (2015) The influence of moisture content on the interfacial properties of natural palm fiber-matrix composite. Wood Sci Technol 49:371–387. https://doi.org/10.1007/s00226-015-0702-3

Manyà JJ, Velo E, Puigjaner L (2003) Kinetics of biomass pyrolysis: a reformulated three-parallel-reactions model. Ind Eng Chem Res 42(3):434–441. https://doi.org/10.1021/ie020218p

Mészáros E, Várhegyi G, Jakab E (2004) Thermogravimetric and reaction kinetic analysis of biomass samples from an energy plantation. Energy Fuels 18(2):497–507. https://doi.org/10.1021/ef034030+

Migneault S, Koubaa A, Erchiqui F, Chaala A, Englund K, Wolcott MP (2011) Application of micromechanical models to tensile properties of wood–plastic composites. Wood Sci Technol 45:521–532. https://doi.org/10.1007/s00226-010-0351-5

Ou R, Zhao H, Sui S, Song Y, Wang Q (2010) Reinforcing effects of Kevlar fiber on the mechanical properties of wood-flour/high-density-polyethylene composites. Compos Part A-Appl S 41:1272–1278. https://doi.org/10.1016/j.compositesa.2010.05.011

Oza S, Ning H, Ferguson I, Lu N (2014) Effect of surface treatment on thermal stability of the hemp-PLA composites: correlation of activation energy with thermal degradation. Compos Part B-Eng 67:227–232. https://doi.org/10.1016/j.compositesb.2014.06.033

Pelaez-Samaniego MR, Yadama V, Lowell E, Espinoza-Herrera R (2013) A review of wood thermal pretreatments to improve wood composite properties. Wood Sci Technol 47:1285–1319. https://doi.org/10.1007/s00226-013-0574-3

Rowell RM (1983) Chemical modification of wood. For Prod Abstr 6:363–382

Saba N, Paridah MT, Jawaid M (2015) Mechanical properties of kenaf fibre reinforced polymer composite: a review. Constr Build Mater 76:87–96. https://doi.org/10.1016/j.conbuildmat.2014.11.043

Saheb DN, Jog JP (1999) Natural fiber polymer composites: a review. Adv Polym Technol 18:351–363. https://doi.org/10.1002/(SICI)1098-2329(199924)18:4%3c351:AID-ADV6%3e3.0.CO;2-X

Tronc E, Hernández-Escobar CA, Ibarra-Gómez R, Estrada-Monje A, Navarrete-Bolaños J, Zaragoza-Contreras EA (2007) Blue agave fiber esterification for the reinforcement of thermoplastic composites. Carbohydr Polym 67:245–255. https://doi.org/10.1016/j.carbpol.2006.05.027

Vuthaluru HB (2004) Investigations into the pyrolytic behavior of coal/biomass blends using thermogravimetric analysis. Bioresour Technol 92:187–195. https://doi.org/10.1016/j.biortech.2003.08.008

Wang X, Liu J, Chai Y (2012) Thermal, mechanical, and moisture absorption properties of wood-TiO_2 composites prepared by a sol–gel process. BioResources 7(1):893–901. https://doi.org/10.15376/biores.7.1.893-901

Wei L, McDonald AG, Freitag C, Morrell JJ (2013) Effects of wood fiber esterification on properties, weatherability and biodurability of wood plastic composites. Polym Degrad Stab 98:1348–1361. https://doi.org/10.1016/j.polymdegradstab.2013.03.027

Wu JH, Hsieh TY, Lin HY, Shiau IL, Chang ST (2004) Properties of wood plasticization with octanoyl chloride in a solvent-free system. Wood Sci Technol 37:363–372. https://doi.org/10.1007/s00226-003-0198-0

Xu C, Leppänen AS, Eklund P, Holmlund P, Sjöholm R, Sundberg K, Willför S (2010) Acetylation and characterization of spruce (*Picea abies*) galactoglucomannans. Carbohydr Res 345:810–816. https://doi.org/10.1016/j.carres.2010.01.007

Yang HP, Yan R, Chen HP, Lee DH, Zheng CG (2007) Characteristics of hemicellulose, cellulose and lignin pyrolysis. Fuel 86:1781–1788. https://doi.org/10.1016/j.fuel.2006.12.013

Yang CN, Hung KC, Wu TL, Yang TC, Chen YL, Wu JH (2014) Comparisons and characteristics of slicewood acetylation with acetic anhydride by liquid phase, microwave and vapor phase reactions. BioResources 9(4):6463–6475. https://doi.org/10.15376/biores.9.4.6463-6475

Yao F, Wu Q, Lei Y, Guo W, Xu Y (2008) Thermal decomposition kinetics of natural fibers: activation energy with dynamic thermogravimetric analysis. Polym Degrad Stab 93:90–98. https://doi.org/10.1016/j.polymdegradstab.2007.10.012

Zhang F, Endo T, Qiu W, Yang L, Hirotsu T (2002) Preparation and mechanical properties of composite of fibrous cellulose and maleated polyethylene. J Appl Polym Sci 84:1971–1980. https://doi.org/10.1002/app.10428